Culicinin D, an Antitumor Peptaibol Produced by the Fungus *Culicinomyces clavisporus*, Strain *LL*-12I252

Haiyin He,*,§ Jeffrey E. Janso,§ Hui Y. Yang,§ Valerie S. Bernan,§ Shuo L. Lin,† and Ker Yu‡

Wyeth Research, 401 N. Middletown Road, Pearl River, New York 10965

Received December 13, 2005

A group of new 10mer linear peptides, designated culicinins A−D (**1**−**4**), was isolated from the fermentation broth of the entomopathogenic fungus *Culicinomyces clavisporus*, strain *LL*-12I252. The structures of the culicinins were determined by a combination of 2D NMR and MS analysis. The major compound, culicinin D (**4**), exhibited selective inhibitory activity against PTEN-negative MDA468 tumor cells. Studies on the 3D structure of **4** using NOE data and computer modeling revealed a dominant conformation of the right-handed helix.

Natural products continue to be important sources for lead compounds in today's drug discovery.[1−3] One of the strategies in enhancing our natural products library is to acquire microorganisms that have not been previously explored by chemical investigation. In addition to depositing extracts of the newly acquired organisms in the library for screening purposes, we also carry out research to examine their secondary metabolites when interesting biological activities are found. As a result of these efforts, we have identified several groups of new compounds, exhibiting bioactivities relevant to our programs.[4,5]

One of the organisms that drew our attention was an entomopathogenic fungus, *Culicinomyces clavisporus*, strain *LL*-12I252, acquired from the ARSEF culture collection in Ithaca, New York. Entomopathogenic fungi, which colonize insect hosts, have been known to be prolific producers of secondary metabolites with diverse structures[6−8] and bioactivities.[9−11] Our studies on 12I252 resulted in the isolation of a group of 10mer linear peptides, designated culicinins A−D (**1**−**4**). The major compound, culicinin D (**4**), was tested in oncology assays and exhibited selective inhibitory activity against PTEN-negative MDA468 breast tumor cells versus PTEN-positive MDA468 cells. Studies on the 3D structure of **4** using NOE constraints and computer modeling revealed a dominant conformation of the right-handed helix. The results of production, structural elucidation, modeling, and biological studies of the culicinins are presented in this paper.

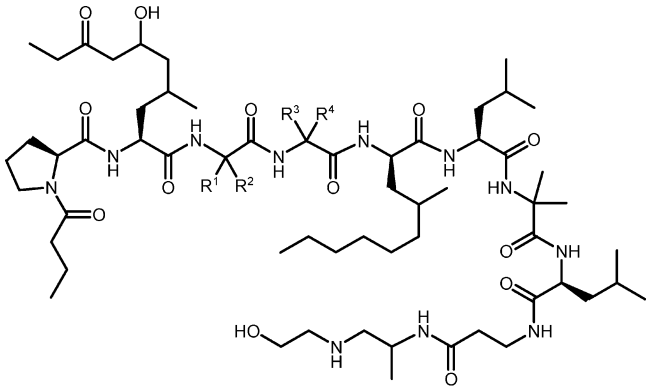

Culicinin A (**1**) $R^1 = R^3 = H$, $R^2 = R^4 = Me$
Culicinin B (**2**) $R^1 = R^2 = R^3 = Me$, $R^4 = H$
Culicinin C (**3**) $R^1 = H$, $R^2 = R^3 = R^4 = Me$
Culicinin D (**4**) $R^1 = R^2 = R^3 = R^4 = Me$

* To whom correspondence should be addressed. E-mail: heh@wyeth.com.
§ Chemical and Screening Sciences.
† Vaccines Research.
‡ Oncology Department.

Results and Discussion

The peptides were produced by fermentation of strain *LL*-12I252 in a liquid medium at 22 °C for 14 days. The organic extract of the whole broth was chromatographed by reversed-phase HPLC to afford a mixture of culicinins A, B, C, and D (**1**−**4**). The predominant component, culicinin D (**4**), purified by further HPLC, showed resolved NMR spectra. These data, together with the MS information, provided the basis for structural determination.

The molecular formula of culicinin D (**4**) was determined to be $C_{63}H_{115}N_{11}O_{13}$ by high-resolution Fourier transform ion cyclotron resonance (FTICR) mass spectrometry (Table 1). The ^{1}H NMR spectrum in C_6D_6 displayed nine signals between δ 8.12 and 9.72, which were assigned by 2D NMR spectroscopic data to amide NH protons. The ^{13}C NMR spectrum contained 10 amide carbonyl signals near δ 170, confirming the peptide structure.

Table 1. HR-FTICRMS Data of Culicinins A−D (**1**−**4**)

compound	composition (MH^+)	observed	required
culicinin A (**1**)	$C_{61}H_{112}N_{11}O_{13}$	1206.8458	1206.8436
culicinin B (**2**)	$C_{62}H_{114}N_{11}O_{13}$	1220.8587	1220.8592
culicinin C (**3**)	$C_{62}H_{114}N_{11}O_{13}$	1220.8588	1220.8592
culicinin D (**4**)	$C_{63}H_{116}N_{11}O_{13}$	1234.8757	1234.8749

Detailed analysis of 2D ^{1}H−^{1}H COSY, TOCSY, ^{1}H−^{13}C HMBC, and HMQC data for compound **4** revealed the presence of eight known amino acids, including two leucines (LEU-1 and -2), a proline (PRO), a 3-aminopropionic acid (APA), three 2-aminoisobutyric acids (AIB-1, -2, and -3), and a 2-amino-6-hydroxy-4-methyl-8-oxodecanoic acid (AHMOD). The presence of AIB residues is a common feature for a class of linear lipopeptides termed peptaibols.[12] These peptides are found exclusively from fungal cultures and are typically composed of a number of nonproteinogenic amino acids. The AHMOD unit was observed for several members of this class, such as leucinostatin A[13] and trichomufins.[14] Further analysis of the NMR data indicated that culicinin D (**4**) contained a butyric acid (BTA) and a 2-(2′-aminopropyl)aminoethanol (APAE), which was previously observed in helioferins[15] and the roseoferin complex.[16] NMR data of culicinin D (**4**) are summarized in Table 2.

In addition to the known building blocks, culicinin D (**4**) contained a new amino acid, 2-amino-4-methyldecanoic acid (AMD), which was initially identified by analysis of spectroscopic data of **4** and then confirmed by isolation. Following the standard acid hydrolysis of **4**, the AMD was isolated by HPLC and its molecular weight was determined to be 201 by ESIMS. The ^{1}H and ^{13}C NMR data of the AMD suggested the presence of a fatty chain, a methyl doublet, a carboxyl group, and an amino group located at the α-position. Several 2D NMR spectra, including COSY, HMBC, and HSQC, helped to delineate the ^{1}H−^{1}H spin system of 2-amino-4-methyldecanoic acid.

10.1021/np058133r CCC: $33.50
Published on Web 04/14/2006

Table 2. NMR Data of Culicinin D (**4**) in C_6D_6

	^{1}H (500 MHz, mult, *J* in Hz)	^{13}C (100 MHz)	HMBC (*J* = 8 Hz)
butyric acid (BTA)			
1		173.82	
2	a. 2.62, b. 2.02 (m)	37.38	C-1, C-3, C-4 (BTA)
3	a. 1.87, b. 1.79 (m)	18.17	C-1, C-2, C-4 (BTA)
4	1.01 (3H, t, 7.3)	13.93	C-2, C-3 (BTA)
proline (PRO)			
1		175.93	
2	4.22 (dd, 8.5, 4)	62.75	C-1, C-3, C-4 (PRO)
3	1.89 (m)	30.18	C-4 (PRO)
	1.77 (m)		
4	2.01 (m)	25.05	C-3 (PRO)
	1.38 (m)		
5	a. 3.83 (dd, 10, 6.4, 6.4)	47.50	C-3, C-4 (PRO)
	b. 2.78 (10, 6.6, 6.5)		
2-amino-6-hydroxy-4-methyl-8-oxodecanoic acid (AHMOD)			
1		176.59	
2	4.59 (ddd, 7.2, 4, 3)	56.49	C-1, C-3 (AHMOD)
2-NH	9.72 (d, 6.1)		C-1 (PRO)
3	2.63 (m)	34.82	C-4, C-4-Me (AHMOD)
	1.42 (m)		
4	2.32 (m)	25.92	C-5, C-6 (AHMOD)
4-Me	1.00 (3H, d, 6.5)	20.60	C-3, C-4, C-5 (AHMOD)
5	1.57 (m)	46.08	C-3, C-4-Me, C-6 (AHMOD)
	1.17 (m)		
6	4.28 (m)	64.45	
7	2.52 (dd, 14, 8)	51.10	C-5, C-6, C-8 (AHMOD)
	2.30 (m)		
8		210.83	
9	2.31 (2H, q, 7.2)	36.86	C-8, C-10 (AHMOD)
10	1.03 (3H, t, 7.2)	7.82	C-8, C-9 (AHMOD)
2-aminoisobutyric acid-1 (AIB-1)			
1		177.49	
2		57.29	
2-NH	9.49 (s)		C-1 (AHMOD), C-2 (AIB-1)
3	1.86 (3H, s)	26.96	C-1, C-2, C-4 (AIB-1)
4	1.72 (3H, s)	23.47	C-1, C-2, C-3 (AIB-1)
2-aminoisobutyric acid-2 (AIB-2)			
1		178.13	
2		56.97	
2-NH	8.75 (s)		C-1 (AIB-1), C-1, C-2, C-3 (AIB-2)
3	1.89 (3H, s)	27.68	C-1, C-2, C-4 (AIB-2)
4	1.71 (3H, s)	23.47	C-1, C-2, C-3 (AIB-2)
2-amino-4-methyldecanoic acid (AMD)			
1		178.04	
2	4.49 (ddd, 10, 5, 5)	56.28	C-1, C-3, C-4 (AMD)
2-NH	8.35 (d, 4.5)		C-1 (AIB-2), C-2, C-3 (AMD)
3	2.59 (m)	39.16	C-1, C-2, C-3, C-4, C-4-Me (AMD)
	2.02 (m)		
4	2.31 (m)	29.55	
4-Me	1.04 (3H, d, 6.5)	18.17	C-3, C-4, C-5 (AMD)
5	1.25−1.40 (2H, m)	38.05	
6	1.25−1.40 (2H, m)	30.28[a]	
7	1.25−1.40 (2H, m)	30.98[a]	
8	1.25−1.40 (2H, m)	32.29	
9	1.31 (2H, m)	23.77	C-8, C-10 (AMD)
10	0.93 (3H, t, 7.0)	14.31	C-8, C-9 (AMD)
leucine-1 (LEU-1)			
1		176.16	
2	4.39 (m)	56.86	C-1, C-3, C-4 (LEU-1)
2-NH	8.83 (d, 5.0)		C-1 (AMD), C-2, C-3 (LEU-1)
3	2.14 (2H, m)	39.76	C-1, C-2, C-4, C-5 (LEU-1)
	2.04		
4	2.05 (m)	25.12	C-2, C-3, C-5 (LEU-1)
5	0.97 (3H, d, 6.5)	22.87	C-3, C-4 (LEU-1)
6	0.96 (3H, d, 6.5)	21.60	C-3, C-4, C-5 (LEU-1)
2-aminoisobutyric acid-3 (AIB-3)			
1		177.49	
2		57.15	
2-NH	8.52 (s)		C-1 (LEU-1), C-1, C-2, C-3 (AIB-3)
3	1.75 (3H, s)	27.85	C-1, C-2, C-4 (AIB-3)
4	1.67 (3H, s)	23.47	C-1, C-2, C-3 (AIB-3)
leucine-2 (LEU-2)			
1		177.14	
2	4.40 (m)	55.96	C-1, C-3, C-4 (LEU-2)
2-NH	8.18 (d, 5.5)		C-1 (AIB-3), C-2, C-3 (LEU-2)
3	2.15 (m)	41.15	C-1, C-2, C-4, C-5, C-6 (LEU-2)
	1.78 (m)		
4	2.08 (m)	25.23	C-2, C-3, C-5, C-6 (LEU-2)
5	1.05 (3H, d, 6.5)	23.17	
6	0.95 (3H, d, 6.5)	22.01	C-3, C-4, C-5 (LEU-2)

Table 2. Continued

	^{1}H (500 MHz, mult, *J* in Hz)	^{13}C (100 MHz)	HMBC (*J* = 8 Hz)
3-aminopropionic acid (APA)			
1		175.66	
2	3.03 (m)	37.74	C-1 (APA)
	2.15 (m)		
3	4.30 (m)	37.39	C-1 (APA)
	3.15 (m)		
3-NH	8.95 (br dd, 7.9, 3.5)		
2-(2′-aminopropyl)aminoethanol (APAE)			
1	3.91 (m)	57.51	
	3.72 (m)		
2	2.87	51.70	
	2.79		
1′	3.68	54.82	C-2′ (APAE)
	2.58		
2′	4.39 (m)	43.40	C-1 (APA)
2′-NH	8.12 (d, 7.9)		C-1 (APA), C-3′ (APAE)
3′	1.08 (3H, d, 7)	17.79	C-1′, C-2′ (APAE)

[a] Assignments may be interchanged.

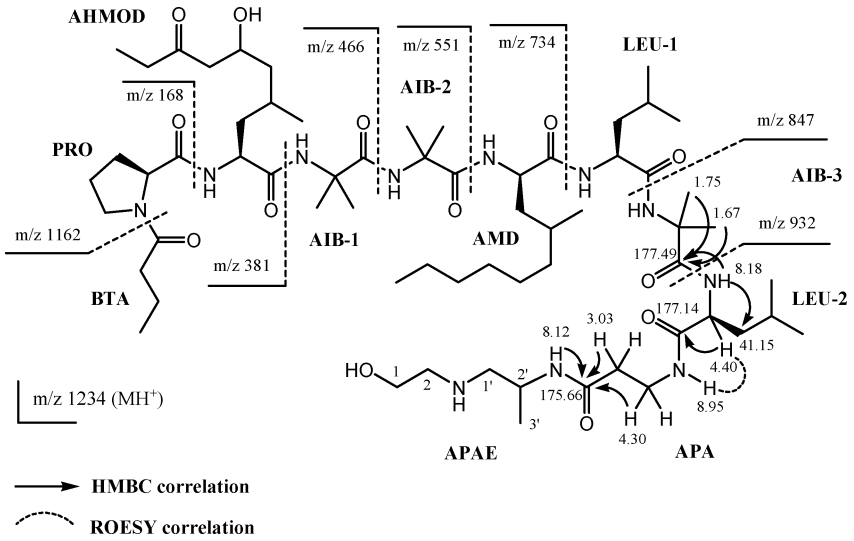

Figure 1. Assignments of ESIMS fragmentation ions and selected 2D NMR data for culicinin D (**4**).

The sequence of these building blocks was established by electrospray ionization mass spectrometry (ESIMS) data. As demonstrated in Figure 1, the fragment ions at *m*/*z* 932, 847, 734, 551, 466, 381, and 168 in an in-source fragmentation spectrum (Figure 2c) clearly indicated the segment BTA-PRO-AHMOD-AIB-AIB-AMD-LEU-AIB-. The connections between amino acids in this segment were also confirmed by 2D NMR spectral data, including two-bond ($^2J_{CH}$) and three-bond ($^3J_{CH}$) correlations in the HMBC spectrum (Table 2) and NOEs in the ROESY spectrum. The remaining sequence, -LEU-APA-APAE-OH, was entirely established by analysis of 2D NMR spectral data, because the fragmentation ions originating from this part of the molecule were lacking.

The building block 2-(2′-aminopropyl)aminoethanol (APAE) was present in several peptaibols. In culicinin D (**4**), the correlations to the C-1 (APA) at δ 175.66 from the 2′-NH (APAE) at δ 8.12 and from the H-2 and H-3 (APA) at δ 3.03 and 4.30 in the HMBC spectrum indicated an amide linkage between the APAE and APA (Figure 1). Furthermore, the correlations to the C-1 (AIB-3) at δ 177.49 from the AIB-3 methyl signals at δ 1.75 and 1.67 and from the NH (LEU-2) at δ 8.18 required a linkage between the LEU-2 and AIB-3. Finally, the connection between the APA and LEU-2 was implied by a strong NOE cross-peak between the 2-NH (APA) at δ 8.95 and H-2 (LEU-2) at δ 4.40 in the ROESY spectrum. The amino acid sequence of culicinin D (**4**) was thus determined to be BTA-PRO-AHMOD-AIB-AIB-AMD-LEU-AIB-LEU-APA-APAE-OH.

The minor components, culicinins A (**1**), B (**2**), and C (**3**), were purified in small quantities by analytical HPLC. The structures of these compounds were elucidated by interpretation of MS data. For culicinin A (**1**), the HR-FTICRMS indicated a molecular formula of $C_{61}H_{111}N_{11}O_{13}$ (Table 1), which was two CH_2's less than culicinin D (**4**). Compared with the ESIMS fragmentation data for D (**4**) (Figure 2c), the fragment ions for **1** at *m*/*z* 904, 819, 706, 523, 452, 381, and 168 (Figure 2a) indicated that the 2-aminoisobutyric acids, AIB-1 and -2, in **4** were both replaced by alanines (ALA) in **1**. The amino acid sequence of **1** was determined to be BTA-PRO-AHMOD-ALA-ALA-AMD-LEU-AIB-LEU-APA-APAE-OH.

The HR-FTICR mass spectrometry data indicated that culicinins B (**2**) and C (**3**) both had a molecular formula of $C_{62}H_{113}N_{11}O_{13}$ (Table 1), which was a CH_2 less than culicinin D (**4**). By comparison of ESIMS fragmentation data of **2** and **3** (Figure 2) with those of **1** and **4**, the respective amino acid sequences of **2** and **3** could unambiguously be established as BTA-PRO-AHMOD-AIB-ALA-AMD-LEU-AIB-LEU-APA-APAE-OH and BTA-PRO-AHMOD-ALA-AIB-AMD-LEU-AIB-LEU-APA-APAE-OH.

Culicinin D (**4**) was hydrolyzed with 6 N HCl at 100 °C, and the absolute stereochemistry of the proteinogenic amino acids was established by derivatization with Marfey's reagent (FDAA) and LC/MS analysis.[17] By comparison with FDAA derivatives of the standard amino acids, the presence of two L-leucines and one L-proline was indicated for **4**. This was consistent with the observation that the chirality of proteinogenic amino acids was L

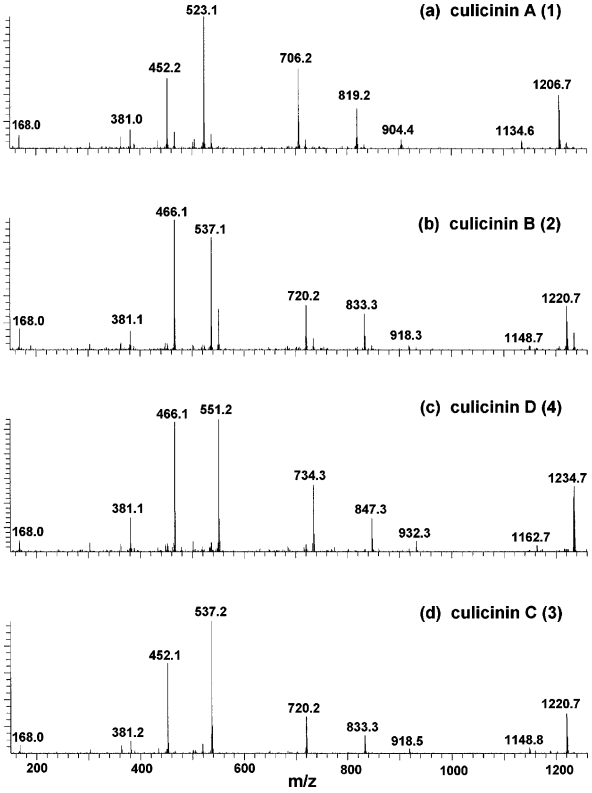

Figure 2. LC/MS data. Finnigan DECA ion trap mass spectrometer, connected to an Agilent 1100 HPLC. ESIMS with in-source fragmentation (positive), sid = 20 v. LC conditions. Column: YMC ODS-A, 2.0 × 100 mm, S-3, 120 Å; solvent: 40−55% MeCN/H_2O with 0.025% formic acid in 19 min, flow rate 0.3 mL/min. (a) Culicinin A (**1**), t_R = 13.76 min. (b) Culicinin B (**2**), t_R = 14.40 min. (c) Culicinin D (**4**), t_R = 14.85 min. (d) Culicinin C (**3**), t_R = 15.57 min.

in almost all peptaibols.[12] In addition, the unusual amino acid AHMOD, characteristic for leucinostatins and the related peptaibols, was also reported to have the L-configuration.[18] We could therefore assume that the AHMOD and AMD in the culicinins were both L-amino acids.

In the NMR analysis of culicinin D (**4**), amide NHs of most amino acids showed no visible exchange with CD_3OD for 3 months at ambient temperature, indicating the presence of a conformation that was stabilized by H-bonding. The 3D structure of **4** was modeled using 11 NOE cross-peaks observed in a ROESY spectrum (Table 3). These NOEs were each detected between a signal of an

Table 3. NOE Distance Restraints of Culicinin D (**4**)

NOE cross-peak[a]	residue 1: proton 1	residue 2: proton 2	intensity	distance bounds (Å)
1	BTA:HA (H-2)[b]	AHMOD:NH	6	1.8−3.7
2	BTA:HA (H-2)[b]	AIB-1:NH	4	1.8−4.7
3	PRO:HD (H-4)[b]	AHMOD:NH	4	1.8−4.7
4	PRO:HA (H-2)	AIB-2:NH	6	1.8−3.5
5	PRO:HA (H-2)	AMD:NH	3	1.8−5.0
6	AHMOD:HA (H-2)	AMD:NH	6	1.8−3.5
7	AHMOD:HA (H-2)	LEU-1:NH	3	1.8−5.0
8	AIB-2:HB (H-3)[c]	AIB-3:NH	3	1.8−5.5
9	AMD:HA (H-2)	LEU-2:NH	6	1.8−3.5
10	AM:D:HA (H-2)	APA:NH	4	1.8−4.5
11	AIB-3:HB (H-3)[c]	APAE:NH	5	1.8−4.5

[a] Observed in a ROESY spectrum acquired on a 500 MHz Bruker instrument (inverse-detected Cryoprobe, C_6D_6 as solvent, mixing time = 250 ms). [b] Methylene. [c] Methyl.

α-proton HA (i) or side-chain protons HB (i) or HD (i) and of a backbone NH (i+*n*, *n* = 1, 2, or 3). Corresponding interproton distance restraints were estimated from the NOE signal intensities.[19] These restraints, together with the observation that culicinin D (**4**) consisted of L-amino acids, virtually defined the conformation of the peptide.

Ten culicinin D (**4**) structural models were generated by simulated annealing computation,[20−22] all satisfying NOE constraints. Consistent with the prevalence of NOE signals detected for (i, i+3) and (i, i+4) residue pairs, all these models showed a right-handed helical conformation (Figure 3). The tighter 3−10 helix conformation was implied at the N-terminus, by the observed (i, i+2) and (i, i+3) NOEs between the proton signals of BTA and of AHMOD and AIB-1.

Most side chains were divergent in conformation among the culicinin D (**4**) models, as they were not constrained during modeling. Despite the divergence, hydrophobic interactions involving the side chains of AIB-1, AIB-2, AIB-3, and LEU-1 apparently contributed to the stabilization of the helical conformation. The presence of a helical conformation in peptaibols with sizes similar to the culicinins, e.g., 10- and 11mers, was previously reported.[23,24]

Biological Activity. Genetic mutation or deletion of the tumor suppressor PTEN is common in human cancer, leading to constitutive signaling of the PI3K/AKT/mTOR pathways.[25] Our previous data[26] indicated that growth of PTEN-negative tumor cells was highly sensitive to inhibition by the mTOR inhibitor CCI-779, whereas the growth of PTEN-positive cells was only minimally inhibited by the drug. Therefore, a cell growth assay employing a pair of tissue-matched breast tumor cell lines MDA468 (PTEN−/−) and MDA435 (PTEN+/+) was used to screen for selective inhibitors that may target components of the PI3K/AKT/mTOR

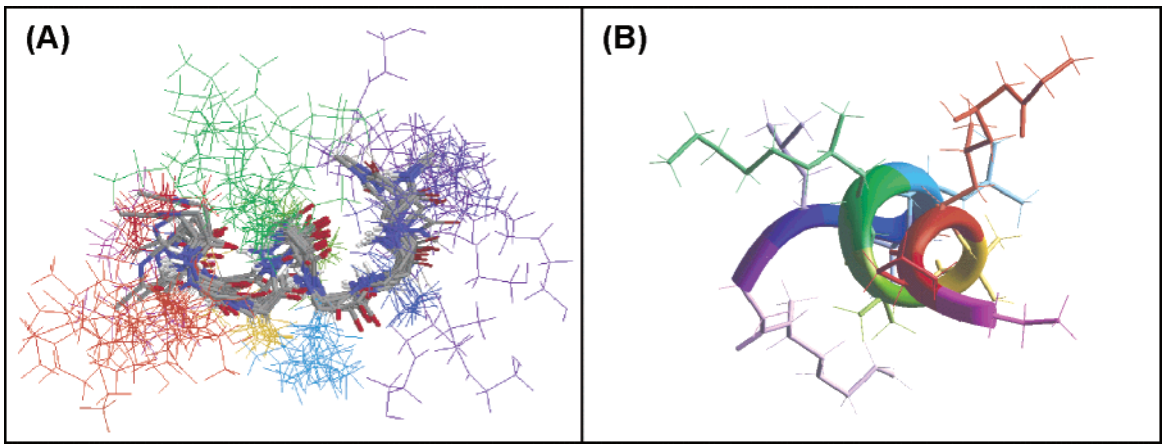

Figure 3. (A) The 10 culicinin D structural models in stick presentation, in which side chains are colored individually, while peptide backbones are drawn thicker and atoms are colored by element: carbon in gray, nitrogen in blue, and oxygen in red. (B) One of the models viewed from the front, in which the backbone is illustrated as a ribbon.

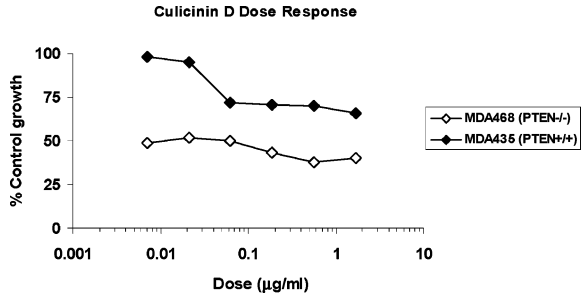

Figure 4. Differential growth inhibition of PTEN−/− MDA468 versus PTEN+/+ MDA435 breast tumor lines by culicinin D (**4**). Cells were plated in 96-well culture plates. After 24 h cells were treated with various concentrations of culicinin D for 3 days. Viable cell numbers from the control and treated groups were determined by a commercial cell proliferation kit as described in General Experimental Procedures.

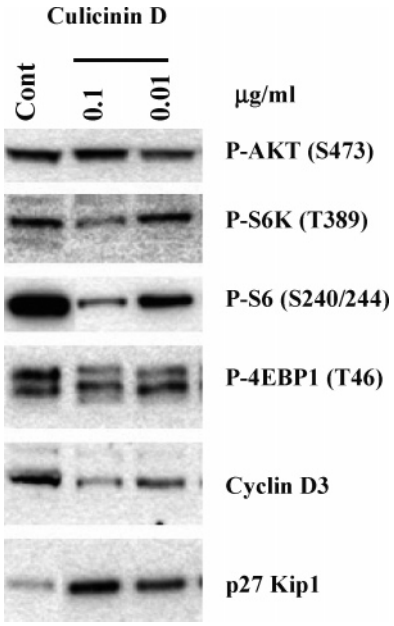

Figure 5. Western blot analysis of MDA468 cells treated with culicinin D (**4**). MDA468 cells were plated in 6-well culture plates. After 24 h cells were treated with culicinin D for 16 h. Total cell lysates were prepared and analyzed by immunoblotting as described in the Experimental Section.

pathway. Culicinin D (**4**) was titrated in the MDA468 versus MDA435 growth inhibition assay. As shown in Figure 4, the compound demonstrated a highly potent but selective inhibition against PTEN−/−MDA468 cells with an IC_{50} value of <0.007 μg/mL. In contrast, its effect on MDA435 cells occurred at significantly higher doses, and an IC_{50} value was not reached at doses as high as 1.6 μg/mL. These data indicated that culicinin D (**4**) may hit a molecular target that is more critically needed in the growth of the PTEN-negative cells, and therefore it may be useful as a selective anticancer agent against PTEN-negative tumors.

To further probe the cellular modulation of biochemical markers in response to inhibition by culicinin D (**4**), we performed a Western blot analysis of MDA468 cells after treatment with 0.1 and 0.01 μg/mL of the compound. In Figure 5, we focused on evaluating the phosphorylation status of several established markers of the PI3K/AKT/TOR pathway. The phosphorylated AKT level was not inhibited, indicating that the PI3-kinase and/or AKT activities were unlikely affected by the treatment. Interestingly, the phosphorylation of mTOR substrates S6K, S6, and 4EBP-1 was inhibited by the treatment in a dose-dependent fashion. Furthermore, consistent with the inhibition of mTOR pathway markers, the compound inhibited cyclin D3, a positive regulator of cell cycle progression, and increased the level of p27 Kip1, an inhibitor of cell cycle. Both cyclin D3 and p27 Kip1 were shown to be similarly modulated by the mTOR inhibitor CCI-779 in these cells.[26] Although the precise mechanism of action for culicinin D (**4**) is unknown, the related leucinostatin A was previously shown to inhibit oxidative phosphorylation in mitochondria.[27] Interestingly, mTOR activity is modulated in cells in response to the integrity and functional status of mitochondria.[28] Collectively, the data suggest that the growth inhibitory action of culicinin D (**4**) may be mediated through the inhibition of the cellular mTOR signaling pathway.

Larger peptaibols with >15 amino acids form stable helical structures due to their hydrophobic amino acid composition, an acylated N-terminus, and the presence of an amino alcohol at the C-terminus. For these peptaibols, oligomerization of the helices facilitates membrane channel formation, and the relationship between this property and their biological activity is well established.[29,30] For smaller peptaibols, however, the membrane activity is decreased, and the mode of action becomes more complex. In some cases, the observed activity could be attributed to a combination of ionophore property and molecular targeting effect.[31] The marked difference between the potencies against MDA468 (PTEN−/−) and MDA435 (PTEN+/+) cells and the modulating activity to the mTOR pathway suggest the presence of specific molecular targets for culicinin D (**4**). A properly designed structure modification may be helpful to reduce the potential membrane toxicity for culicinins as well as for smaller peptaibols in general.

Experimental Section

General Experimental Procedures. The majority of 1D and 2D NMR data was recorded on a Bruker DPX-400 spectrometer at 400 and 100 MHz for ^1H and ^{13}C, respectively, using a 3 mm broadband probe. HSQC was optimized at $^1J_{C-H} = 140$ Hz, and HMBC, optimized at $^nJ_{C-H} = 8.3$ Hz. The 2D ROESY spectrum was acquired on a Bruker DRX 500 MHz instrument, equipped with a 3 mm inverse-detected Bruker Cryoprobe (mixing time = 500 ms). High-resolution Fourier transform ion cyclotron resonance mass spectrometry data were acquired on a Bruker APEXII FTICR mass spectrometer, equipped with a shielded 9.4 T superconducting magnet. ESIMS data with in-source fragmentation (positive) were recorded on a Finnigan DECA ion trap mass spectrometer.

Fungal Strain. Strain *LL*-12I252 was obtained from the ARSEF culture collection in Ithaca, NY, as ARSEF 2481. This organism was isolated from larva of *Forcipomyia marksae* collected in Millaa, Queensland, Australia, and identified to be a strain of *Culicinomyces clavisporus* by Stephen P. Frances (Australian Army Malaria Institute). Strain *LL*-12I252 was cultured on Bennett's medium (10 g of dextrose, 0.77 g of beef extract, 1.0 g of yeast extract, 2.0 g of NZ-amine, and 15.0 g of agar per liter of distilled water). After three weeks' incubation at 22 °C, conidiophores and conidia were present. The conidia were ovate and developed from flask-shaped phialides with swollen bases. The phialides were present singly and in whorls.

Fermentation. Strain *LL*-12I252 was plated onto Bennett's medium from frozen stock and was incubated at 22 °C until there was sufficient mycelial growth to inoculate into the first stage seed. The culture was transferred into 25 × 150 mm tubes, each containing 11 mL of Difco potato-dextrose broth (PDB). The seed tubes were shaken at 160 rpm at 22 °C. After 4 days of incubation, the seed cultures were inoculated into production: three 2.8 L Fernbach flasks each containing 1 L of PDB with shaking at 200 rpm and 22 °C. Production of culicinins was monitored by testing the whole broth for inhibition of methicillin-sensitive *S. aureus* via the agar diffusion method.[32] The fermentations were harvested on the 14th day of incubation.

Isolation of Culicinins A−D (1−4). The whole broth was centrifuged at 3800 rpm at 22 °C. The supernatant and pellet were respectively extracted with n-BuOH (2 × 1.5 L) and MeOH (2 × 0.5 L). The combined extract was then evaporated under reduced pressure to give a grayish gum, which was then chromatographed by preparative reversed-phase HPLC. The column was an YMC ODS-A, 70 × 500 mm in size, 10 μm particle size, 120 Å. The solvent was a linear gradient of 60−100% MeCN/H_2O, both containing 0.01% TFA, in 40

min. A broad peak, monitored by UV at 210 nm, at ~29 min was collected. Upon evaporation, it gave a colorless oily peptide mixture (125 mg). This mixture was analyzed by LC/MS to contain four peptides (**1**−**4**), with a ratio of ~2:1:2:20 according to UV absorption at 210 nm. The major component, D (**4**), was further purified by reversed-phase HPLC (column: YMC ODS-A, 30 × 250 mm, 5 μm, 120 Å; solvent: 40−100% with 0.01% TFA in 30 min) as a colorless glass (15.6 mg). High-resolution FTICR MS and NMR data, see Tables 1 and 2.

2-Amino-4-methyldecanoic Acid (AMD). The culicinin mixture (**1**−**4**, 115 mg) was dissolved in 6 N HCl (500 mL), and the solution was stirred at 100 °C for 16 h. After cooling, the hydrophobic hydrolysate was extracted by n-BuOH (100 mL), evaporated, and chromatographed by HPLC. Column: YMC ODS-A, 30 × 250 mm, 5 mm, 120 Å. Solvent: 15−100% MeCN/H_2O (0.01% TFA) over 23 min, 20 mL/min. The peak at 13 min, monitored at 210 nm, was evaporated to give AMD as a colorless oil (7.5 mg): ^{1}H NMR (400 MHz, DMSO-d_6, mult, J in Hz) δ 3.78 (m, H-2), 1.50−1.65 (3H, m, H_2-3, H-4), 1.23 (9H, m, H-5, H_2-6, -7, -8, -9), 1.12 (m, H-5), 0.86 (3H, d, 6.5), 0.84 (3H, t, 6.5); ^{13}C NMR (100 MHz, DMSO-d_6) δ 171.67 (C-1), 50 66 (C-2), 37.76 (C-3), 36.36 (C-5), 31.32 (C-8), 28.90 (C-7), 28.27 (C-4), 26.09 (C-6), 22.13 (C-9), 18.84 (4-CH_3), 14.00 (C-10); ESIMS m/z 202.1 (MH^+).

Absolute Configuration of Amino Acids. Culicinin D (**4**, 1.0 mg) was dissolved in degassed 6 N HCl (0.5 mL) and heated at 105 °C for 15 h. The solvent and acid were evaporated under reduced pressure, and the residue was dried under high vacuum. An aqueous solution of the hydrolysate (0.1 mL) was treated with 1% 1-fluoro-2,4-dinitrophenyl-5-L-alanineamide (FDAA) in acetone (0.1 mL) and 6% triethylamine in H_2O (30 μl) at 40 °C for 1 h.[17] The reaction mixture was diluted with 1:1 MeCN/H_2O (0.2 mL) and then analyzed by HPLC on an YMC ODS-A column (3 μm, 120 Å, 2.0 × 100 mm). The solvent was a linear gradient of 20−70% MeCN/H_2O with 0.025% formic acid in 18 min (flow rate, 0.3 mL/min). The mobile phase was monitored by both UV absorption at 254 nm and negative ESIMS. The retention times in minutes and the negative ions, $(M - H)^-$, are given in parentheses: L-proline (9.5, 365.9) and L-leucine (12.0, 381.8). The retention times were consistent with the FDAA derivatives of the commercial samples, L-proline and L-leucine.

Structural Modeling. The program X-PLOR[20] was used to model the 3D structure of culicinin D (**4**) by distance-constraint simulated annealing. Eleven distance restraints were derived from ^{1}H−^{1}H interresidual NOE cross-peaks in a ROESY spectrum. The intensities of these peaks were measured by contour levels ranging from 3 to 6, out of a maximum of 12. They were converted to distance upper bounds of 3.5−5.0 Å, which were compensated for degenerate methylene and methyl signals. The distance lower bound was kept constant at 1.8 Å. Simulated annealing was conducted following an established protocol.[21] Briefly, a crude model was built manually and submitted to a molecular dynamics cycle of heating (from 50 to 1000 K), equilibrium, production, and cooling (from 1000 to 100 K), followed by energy minimization. Strengths of NOE restraints and various energy terms were adjusted during different stages of dynamics simulation. Ten such cycles were conducted to produce 10 individual models, each satisfying the given distance restraints. Quality of the models was verified by PROCHECK.[22] Illustrations of the model structures were generated by the programs RasMol (http://openrasmol.org) and InsightII (Accelrys, San Diego, CA).

Cell Growth Assay. Human breast tumor cells, MDA468 and MDA435, were plated in 96-well culture plates. One day following the plating, culicinin D (**4**) was added to the cells at the indicated concentrations. Three days after the drug treatment, viable cell densities were determined by metabolic conversion (by viable cells) of the dye MTS, a well-established cell proliferation assay. The assays were performed using an assay kit purchased from Promega Corp. (Madison, WI) following the protocol supplied with the kit. The MTS assay results were read in a 96-well plate reader by measuring absorbance at 490 nm. The effect of each treatment was calculated as percent of control growth relative to the vehicle-treated cells grown in the same culture plate.

Western Blot Analysis. MDA468 cells were plated in 6-well culture plates. Twenty-four hours later, cells were treated with indicated doses of culicinin D (**4**) for 16 h in full growth media. Protein lysates were prepared for Western blot analysis as previously described.[26]

Acknowledgment. The authors wish to thank Drs. L. McDonald for the ROESY spectrum, X. Feng for high-resolution MS data, and L. Toral-Barza, D. Roll, M. Singh, F. Koehn, and G. Carter for helpful discussions.

References and Notes

(1) Berdy, J. *J. Antibiot.* **2005**, *58*, 1−26.
(2) Koehn, F. E.; Carter, G. T. *Nat. Rev. Drug Discovery* **2005**, *4*, 206−20.
(3) Newman, D. J.; Cragg, G. M.; Snader, K. M. *J. Nat. Prod.* **2003**, *66*, 1022−37.
(4) He, H.; Janso, J. E.; Williamson, R. T.; Yang, H. Y.; Carter, G. T. *J. Org. Chem.* **2003**, *68*, 6079−82.
(5) He, H.; Janso, J. E.; Yang, H. Y.; Singh, M. P.; Bernan, V. S.; Greenstein, M.; Carter, G. T. *J. Antibiot.* **2002**, *55*, 821−5.
(6) Kikuchi, H.; Miyagawa, Y.; Sahashi, Y.; Inatomi, S.; Haganuma, A.; Nakahata, N.; Oshima, Y. *Tetrahedron Lett.* **2004**, *45*, 6225−8.
(7) Kikuchi, H.; Miyagawa, Y.; Nakamura, K.; Sahashi, Y.; Inatomi, S.; Oshima, Y. *Org. Lett.* **2004**, *6*, 4531−3.
(8) Namphung, V.; Prasat, K.; Masahiko, I.; Srisuda, T.; Saovaluk, V.; Morakot, T.; Yodhathai, T. *J. Nat. Prod.* **2002**, *65*, 1346−8.
(9) Nam, K. S.; Jo, Y. S.; Kim, Y. H.; Hyun, J. W.; Kim, H. W. *Life Sci.* **2001**, *69*, 229−37.
(10) Nilanonta, C.; Isaka, M.; Kittakoop, P.; Saenboonrueng, J.; Rukachaisirikul, V.; Kongsaeree, P.; Thebtaranonth, Y. *J. Antibiot.* **2003**, *56*, 647−51.
(11) Schmidt, K.; Guenther, W.; Stoyanova, S.; Schubert, B.; Li, Z.; Hamburger, M. *Org. Lett.* **2002**, *4*, 197−199.
(12) Degenkolb, T.; Berg, A.; Gams, W.; Schlegel, B.; Graefe, U. *J. Pept. Sci.* **2003**, *9*, 666−78.
(13) Mori, Y.; Tsuboi, M.; Suzuki, M.; Fukushima, K.; Arai, T. *J. Antibiot.* **1982**, *35*, 543−4.
(14) Berg, A.; Grigoriev, P. A.; Degenkolb, T.; Neuhof, T.; Haertl, A.; Schlegel, B.; Graefe, U. *J. Pept. Sci.* **2003**, *9*, 810−6.
(15) Graefe, U.; Ihn, W.; Ritzau, M.; Schade, W.; Stengel, C.; Schlegel, B.; Fleck, W. F.; Kuenkel, W.; Haertl, A. Gutsche, W. *J. Antibiot.* **1995**, *48*, 126−33.
(16) Degenkolb, T.; Heinze, S.; Schlegel, B.; Dornberger, K.; Mollmann, U.; Dahse, H.-M.; Grafe, U. *J. Antibiot.* **2000**, *53*, 184−190.
(17) Fuji, K.; Ikai, Y.; Oka, H.; Suzuki, M.; Harada, K.-i. *Anal. Chem.* **1997**, *69*, 5146−51.
(18) El Hadrami, M.; Lavergne, J. P.; Viallefont, P.; Itto, M. Y. A.; Hasnaoui, A. *Tetrahedron Lett.* **1991**, *32*, 3985−8.
(19) Megy, S.; Bertho, G.; Gharbi-Benarous, J.; Baleux, F.; Benarous, R.; Girault, J. P. *Peptides* **2005**, *26*, 227−41.
(20) Brunger, A. T. *X-PLOR Version 3.1*, A system for X-ray crystallography and NMR; Yale University Press: New Haven, CT, 1992.
(21) Nilges, M.; Clore, G. M.; Gronenborn, A. M. *FEBS Lett.* **1988**, *229*, 317−24.
(22) Laskowski, R. A.; MacArthur, M. W.; Moss, D. S.; Thornton, J. M. *J. Appl. Crystallogr.* **1993**, *26*, 283−91.
(23) Auvin-Guette, C.; Rebuffat, S.; Prigent, Y.; Bodo, B. *J. Am. Chem. Soc.* **1992**, *114*, 2170−4.
(24) Cerrini, S.; Lamba, D.; Scatturin, A.; Ughetto, G. *Biopolymers* **1989**, *28*, 409−20.
(25) Vivanco I.; Sawyers C. L. *Nat. Rev. Cancer* **2002**, *2* (Jul), 489−501.
(26) Yu, K.; Toral-Barza, L.; Discafani, C.; Zhang, W. G.; Skotnicki, J.; Frost, P.; Gibbons, J. J. *Endocr. Relat. Cancer* **2001**, *8* (Sep), 249−58.
(27) Shima, A.; Fukushima, K.; Arai, T.; Terada, Hi. *Cell Struct. Funct.* **1990**, *15*, 53−8.
(28) Kim, D.-H.; Sarbassov, D. D.; Ali, S. M.; King, J. E.; Latek, R. R.; Erdjument-Bromage, H.; Tempst, P.; Sabatini, D. M. *Cell* (*Cambridge, Mass.*) **2002**, *110*, 163−75.
(29) Chugh, J. K.; Bruckner, H.; Wallace, B. A. *Biochemistry* **2002**, *41*, 12934−41.
(30) Duclohier, H.; Wroblewski, H. *J. Membr. Biol.* **2001**, *184*, 1−12.
(31) Csermely, P.; Radics, L.; Rossi, C.; Szamel, M.; Ricci, M.; Mihaly, K.; Somogyi, J. *Biochim. Biophys. Acta, Mol. Cell Res.* **1994**, *1221*, 125−32.
(32) Singh, M. P.; Greenstein, M. *Curr. Opin. Drug Discovery Dev.* **2000**, *3*, 167−76.

NP058133R